Contribution of the spreading resistance to high-frequency rectification in metal-metal point contacts

R. W. van der Heijden, H. M. Swartjes, and P. Wyder
Research Institute for Materials, University of Nijmegen, Toernooiveld, 6525 ED Nijmegen, The Netherlands

(Received 4 October 1982; accepted for publication 23 September 1983)

High-frequency radiation detection by metal-metal point contacts is investigated as a function of bias voltage at far-infrared frequencies. Detection occurs through rectification due to a nonlinearity of the current-voltage characteristic. The relative contribution to the rectification due to an electron phonon scattering mechanism occurring in the bulk material ("spreading resistance") is compared with other mechanisms. The spreading resistance nonlinearity was identified by measurements at liquid helium temperatures. For low contact resistances ($\lesssim 50\ \Omega$) this nonlinearity was generally dominant, for higher resistances it may occur in addition to and independently of the other mechanisms.

PACS numbers: 73.40.Jn, 73.40.Cg, 71.38 + i, 72.30. + q

I. INTRODUCTION

Point-contact diodes are by now very well established nonlinear devices to be used for harmonic generation and mixing at infrared and near-visible frequencies. This enables accurate measurement of laser frequencies which is of great importance for spectroscopy and metrology.[1] The point contact consists of a fine wire, sharpened to a small point, which is gently brought into electrical contact with another conductor. The wire acts as an antenna when exposed to a radiation field[2] so that high-frequency currents are generated across the contact, which is supposed to have a nonlinear current-voltage characteristic.

A point contact between superconductors (forming a Josephson junction) or between a metal and a semiconductor may be used (including the photolithographically fabricated Schottky diode, but at the highest frequencies only a simple contact between metals at room temperature has proven to be successful.[3] A great deal of work exists which deals with the origin of the nonlinearity in metal-metal contacts. An elucidation of the operation mechanism of the nonlinear diodes as far as possible is important as this may serve as a guide to device optimization.

To explain the nonlinearity in room temperature metal-metal contacts, the most widely adopted model is that a thin insulating layer at the interface causes a nonlinear tunneling barrier.[4,5] For this reason, one usually refers to these junctions as metal-insulator-metal (MIM) junctions (or MOM, where O stands for oxide). Recently, the tunneling theory was extended and refined by an improved calculation of the barrier potential and taking into account effects of geometrical asymmetry and asymmetric heating of both electrodes.[6] Experimental evidence for the importance of these effects seems to become available.[7] In addition, the earlier methods of calculating the nonlinear current-voltage (I-V) characteristics originating from electron tunneling are subject to criticism.[8] At high frequencies still other effects have been observed or proposed to be of importance, like photoexcitation of electrons,[9] resonant interband transitions[10] or surface plasmons.[11]

The general major obstacle for a detailed and reliable analysis of practical high-frequency point contact diodes is that the microscopic nature of the contact is very difficult to characterize and even more difficult to control. Because calculations of high frequency behavior based on the tunneling mechanism depend rather strongly on poorly known parameters (shape and thickness of barrier, point contact geometry, temperature difference, amplitude of induced high-frequency voltage, etc.) an unambiguous comparison of theory and experiment is difficult to make. Consistent with these problems is the fact that experimentally a widely varying range of behavior is also found.

Recently, we have investigated the rectification behavior of normal metal point contacts at far-infrared (FIR) frequencies and liquid helium (LHe) temperatures.[12] High frequency investigations of MIM diodes at low temperatures scarcely exist, obviously because low temperature operation presents a considerable inconvenience for practical use. It was found[12] that the rectification for not too high resistance contacts at finite bias voltage was completely dominated by a nonlinearity due to an electron phonon scattering process occurring in the bulk material.[13,14] This nonlinearity is well understood and because it results from a bulk process, it is not very dependent on the detailed nature of the contact. The contribution to the point contact resistance resulting from the bulk electrodes is commonly referred to as the spreading resistance.

The purpose of the present paper is to investigate the relative importance of the nonlinear spreading resistance as compared to other mechanisms for the nonlinearity for a rather general metal-metal contact. Therefore the rectification and nonlinearity was measured as a function of bias voltage for a series of contact resistances, for varying temperatures and for different electrode materials. The conclusion is that for high resistances (larger than several hundred ohm) the spreading resistance nonlinearity is no longer dominant. We will finally discuss whether those contacts, where the magnitude of the spreading resistance nonlinearity is optimized, might be of any practical use.

After description of some experimental details, the

 0021-8979/84/041003-09$02.40

physical mechanism for the nonlinearity and the principle of high-frequency operation will be briefly recalled. Then, the experimental results will be presented and discussed.

II. EXPERIMENTAL DETAILS

As the present experiments were aimed at investigating the detection mechanism only, no elaborate coupling scheme has been employed. An outline of the experimental configuration is given in Fig. 1. The point contact was mounted at the end of a 13-mm-diameter stainless-steel light pipe which ended in a small angle copper cone of 4 mm final diameter. The light pipe system was placed in a standard glass dewar which can be filled with liquid helium, so that the point contact was directly surrounded by the helium (see Fig. 1). The helium bath can be pumped down to ~ 1.5 K.

Radiation from a standard type optically pumped (CO_2 laser) far-infrared waveguide laser was led to the junction by ~ 1.5-m total length light pipe. The power level at the laser output was in the mW range but was attenuated if desired. Laser-induced signals were phase sensitively detected, with the CO_2 laser beam chopped at 560 Hz. A low noise selective preamplifier (PAR 113) was used in front of the lock-in amplifier, optionally preceeded by an impedance matching transformer (PAR AM1). Signals were recorded as a function of dc bias voltage. Because of the distorting effects of light pipe and cone, the radiation was unfocussed and unpolarized at the location of the contact.

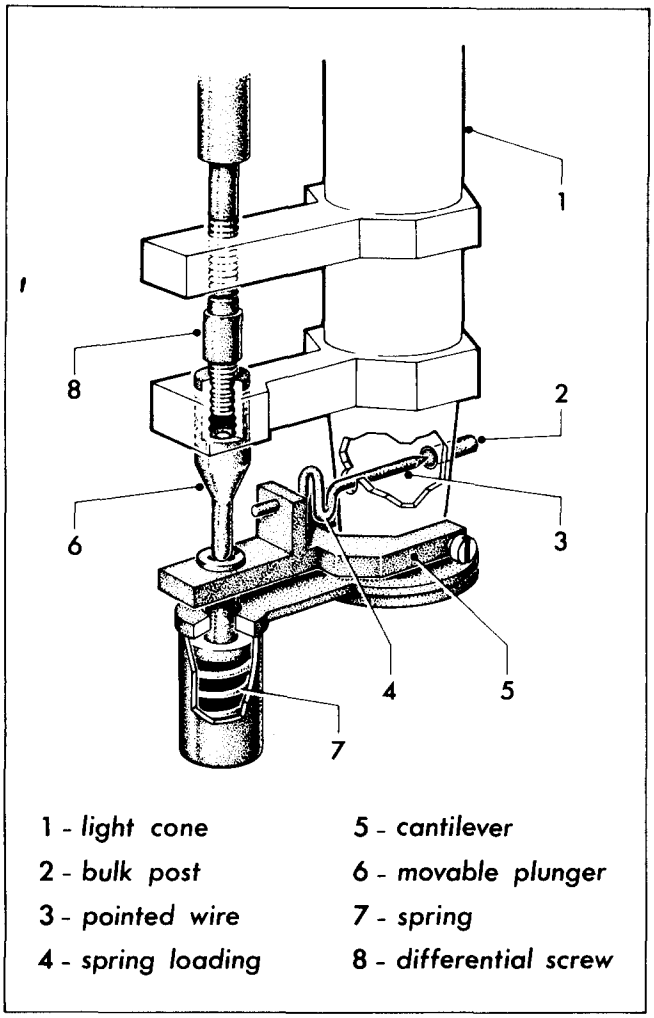

FIG. 1. Detail of point contact mounting at the lower end of the light pipe.

The pointed wire could be adjusted from top of the dewar using a differential screw assembly in combination with a cantilever mechanism. Adjustment accuracy corresponds to 25 μm per shaft turn. Suitable contacts were made by a combination of mechanical adjustment and electrical sparking following a trial and error method. It was found experimentally that the magnitude of the detected signal did not depend much on the location of the contact along a diameter of the cone. Mostly, the post was situated with its front face approximately along the cone sidewall. An S-shaped spring was bent in the whisker, intended to provide somewhat improved mechanical stability. Special precautions, necessary to maintain a given contact over an extended temperature range,[15] were not available with the present setup. Therefore in the temperature dependence measurements, the contacts were readjusted at each temperature.

Copper of normal, electrical grade quality was used for the whisker and post. The whisker tip was made by standard electrolytical etching. The post was usually only etched in HNO_3 and occasionally mechanically polished. Polishing however turned out to be not very important and was usually omitted. Good results could be obtained with a surface that looked even somewhat rough to the bare eye.

Current-voltage characteristics and its first and second derivatives dV/dI and d^2V/dI^2 were measured using a standard current modulation technique and bridge circuit, the same as that used in other work.[13,14]

III. THEORETICAL BACKGROUND

The most important parameter characterizing the contact is the contact area. As usual, it will be assumed circular, with diameter a. A further characterization is given by distinguishing two limiting cases: (1) Constriction-type contacts. The electrodes are in good metallic contact without a physical barrier between them (conducting hole in an insulating screen mode).[14] (2) Tunnel-type contacts. A physical barrier (insulating layer) exists at the interface, so that electron tunneling is responsible for current transport. Although in real cases there will be a gradual transition from constriction- to tunnel-type contacts, for the present purpose it suffices to distinguish the limiting cases only.

Independent of the contact nature, the resistance contribution due to current flowing in the bulk electrodes is given by the Maxwell resistance or spreading resistance R_s (Refs. 14 and 16):

$$R_s = \rho/2a, \tag{1}$$

where ρ is the resistivity of the metal. For tunnel-type contacts, the tunneling resistance is denoted by R_T and current transport results from field emission, as the Fermi level has the familiar step across the insulating layer. The step height is eV where e is the electron charge and V the potential drop. A similar picture holds for the constriction contact, provided that the electronic mean free path l is much larger than

the contact diameter.[14] Because the electric field is confined to a region within the electron mean free path, the energy acquired after traversing the constriction equals eV. This process is properly called field emission as well.[14] The constriction resistance for a very small ($a \ll l$) constriction, here denoted by R_{FE}, is given by the Sharvin expression.[17] $R_{FE} = 4l\rho/3\pi a^2$. The resistance for a constriction with arbitrary hole radius is given by a weighted sum of R_s and R_{FE}.[14] The weighting factor, which is of the order of unity, is not essential for a qualitative discussion. Comparing a small constriction and tunnel contact of otherwise identical geometry, we have $R_T = R_{FE}/D$, where D is the electron tunneling probability in case of the tunneling junction. For both types of field emission we require $R_s \ll R_{FE}$, $R_s \ll R_T$.

The nonlinearity of R_s under field emission conditions arises because of the energy dependence of the scattering time τ, which determines ρ in Eq. (1) in the usual manner. This nonlinearity was extensively studied and recently reviewed.[14] The most familiar process rendering τ energy dependent, and relevant to the present work is electron phonon interaction. This is demonstrated experimentally by the fact that R_s shows a relatively steep rise (or peak in d^2V/dI^2) at energies eV corresponding to the zone boundary acoustic phonons of the electrode material[14] (for Cu: 17 and 28 meV).

In a semiclassical, microscopic theory,[14,18] the nonlinearities arise as first-order corrections to a linear field emission term. The separation of the total resistance into a constant term (R_{FE} or R_T) and a voltage dependent term (R_s) seems therefore still justified from a microscopic point of view. The discussion of the nonlinear spreading resistance in the present work will be based upon the theoretical interpretation and analysis used in the earlier work.[14,18]

To interpret high frequency behavior of point-contact diodes (including Schottky diodes) a simple equivalent circuit representation such as given in Fig. 2 is frequently used.[19–22] The point-contact wire which acts as an antenna is represented by a voltage source of amplitude V_a with resistance R_a. A typical value for R_a in the far infrared is 150 Ω (Ref. 21). The junction is represented by a contact resistance R_b in series with the spreading resistance R_s, accounting for the bulk contribution to the resistance. To account for a high-frequency cutoff, R_b is usually shunted by a capacitance C. From the preceeding discussion, it seems reasonable to use this standard circuit also for the high-frequency behavior associated with R_s. For a tunneling junction $R_b = R_T$ and for a small constriction junction $R_b = R_{FE}$ as defined before.

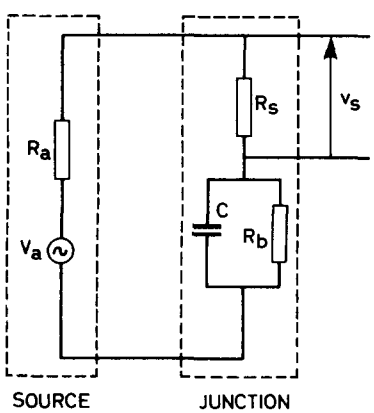

FIG. 2. Equivalent network for analyzing the point contact detection.

In all existing models of MIM junctions (as well as Schottky diodes) the nonlinearities are attributed to R_b (e.g., the tunneling process) while R_s is assumed to be a constant. For some configurations and frequency ranges R_s may determine the high frequency cutoff, when $1/\omega C$ becomes smaller than R_s (Ref. 19). The present work on the other hand will be concerned with a nonlinear R_s. Models describing nonlinearities in R_b will not be discussed explicitly. This main nonlinearity of R_s has a very specific structure at low temperatures, characteristic for the electrode material, so that this nonlinearity can be unambiguously identified. Other nonlinearities are not very reproducible, depend strongly on the contact parameters, and occur predominantly in high-resistance contacts. These obviously result from the interface and should therefore be attributed to R_b. It is the purpose of the present work to determine experimentally roughly the range of conditions for which the nonlinearity of R_s may be significant compared to the nonlinearity of R_b.

A useful measure for the nonlinearity of a resistance R is the logarithmic slope S:

$$S = (1/R)(dR/dV) \equiv (d^2I/dV^2)/(dI/dV). \tag{2}$$

When used as a rectifier, the voltage sensitivity, defined as the dc-induced voltage per unit power absorbed is then in the small power limit given by $\frac{1}{2}SR$. Formally, because we assume R_s to be the only nonlinear resistance, the rectified voltage V_{dc} would be given by $V_{dc} = \frac{1}{2}S'R_sP_s$ with $S' \equiv (1/R_s)(dR_s/dV')$, the nonlinearity parameter associated with R_s only and P_s the high-frequency power dissipated in R_s. $P_s \cong V_s^2/2R_s$ with V_s high-frequency voltage amplitude across R_s. The derivative is with respect to the voltage V' across R_s. It is however easily seen that V_{dc} is equally well expressed as $V_{dc} = \frac{1}{2}SR_tP_j$. Here, we neglect C, $R_t = R_s + R_b$, P_j is the total power dissipated in the junction (in R_s and R_b), and S is the nonlinearity as measured from the junctions I-V characteristics: $S \equiv (1/R_t)(dR_t/dV)$.

The nonlinearity parameters arising from the nonlinear spreading resistance in case of a tunneling junction S_T and a small constriction junction S_c, both having the same resistance R_t, have been compared earlier[14] with the result:

$$S_T(R)/S_c(R) = D^{1/2}. \tag{3}$$

(It is assumed implicitly that the oxide thickness is small, so that geometric effects are the same in both cases.) As follows from Eq. (3), the nonlinearity of a tunneling junction is smaller by a factor $D^{1/2}$ than that of a constriction junction having the same resistance, despite the larger contact area of such a tunneling junction. For the point contact spectroscopy experiments[14] relatively low-resistance, small-constriction type contacts are therefore preferably selected.

For R_s to be nonlinear, it is essential that the electrons are injected into the bulk at energy eV, obtained by traversing the voltage drop across R_b. The circuit of Fig. 2 therefore cannot be reliable when R_b is shorted by C. The final expression for the induced voltage will therefore be given at low

frequencies ($\omega CR_b < 1$), yielding the simple result:

$$V_{dc} = \tfrac{1}{2} SR_t \left(\frac{4R_a R_t}{(R_a + R_t)^2} \right) P_a . \quad (4)$$

P_a is the power received by the antenna and the factor in large parentheses is the fraction of this which is dissipated in the junction.

IV. EXPERIMENTAL RESULTS

A. Low resistance contacts at low temperature

The upper trace of Fig. 3(a) shows the second derivative (d^2V/dI^2) of the I-V characteristic of a Cu-Cu point contact at liquid helium temperature. The main peak at 17 meV corresponds to the typical phonon energies in Cu and results from electron-phonon interaction.[14] The two lower curves display the laser-induced voltage as a function of bias voltage, taken at low laser power for two different laser frequencies. For a low resistance contact, a high-frequency current bias $i = i_0 \cos \omega t$, ω laser frequency, can be assumed, so that the induced dc voltage is given by $V_{det} = \frac{1}{4} (d^2V/dI^2) i_0^2$. V_{det} therefore is directly proportional to d^2V/dI^2 and independent of frequency, in agreement with the observations. The behavior shown in Fig. 3(a) is typical for a small constriction contact: all nonlinearity can be attributed to the spreading resistance. The modulation current amplitude i_0 or voltage amplitude v_0 can be estimated from the measured V_{det} and d^2V/dI^2. An independent check of the modulation amplitude may be obtained from measurements as a function of power [see Fig. 3(b)]: when the high-frequency voltage swing v_0 becomes comparable to the width of the peak in d^2V/dI^2, the structure becomes broadened and smeared out. Figure 3 summarizes the results, essentially reported earlier.[12]

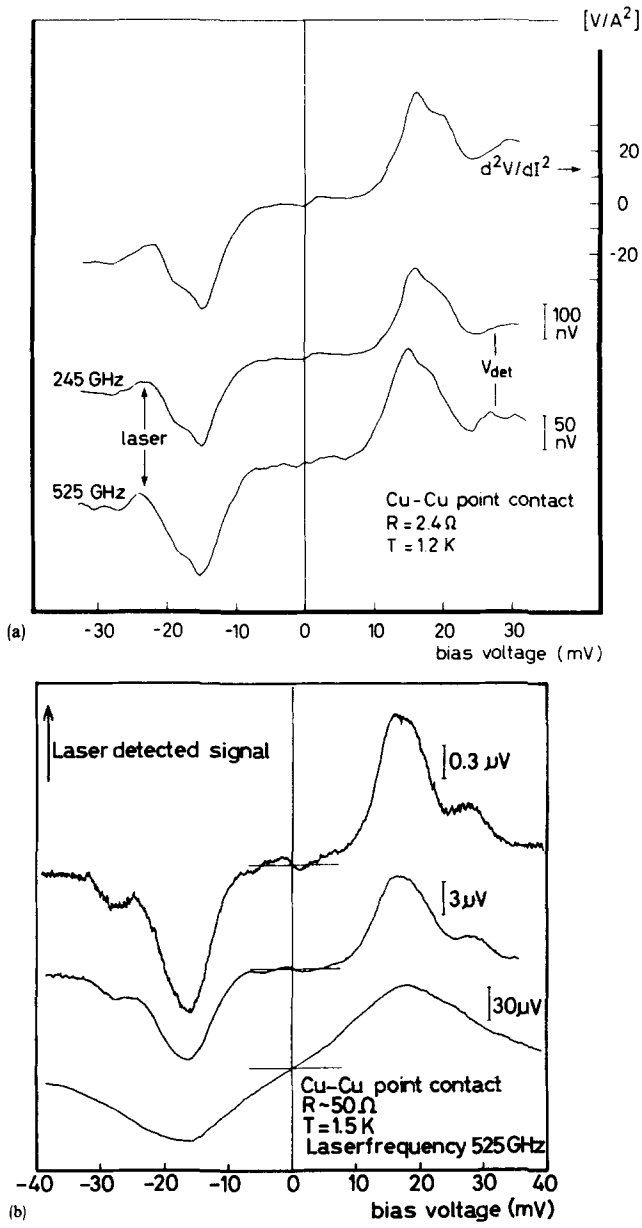

FIG. 3. (a) Second derivative (d^2V/dI^2) (upper curve) and laser-induced signal (V_{det}) for two laser frequencies (lower two curves) as a function of bias voltage. (b) Laser-detected signal curves for a sensitive (high ohmic) point contact for three different laser powers, showing the effect of power broadening.

Two examples of rectification by contacts with a d^2V/dI^2 curve different from the simplest one [Fig. 3(a)], are shown in Fig. 4. One contact has a large "zero bias anomaly" (large d^2V/dI^2 at low bias voltage), and the other has a large "background" (large d^2V/dI^2 at large bias voltages). Both contacts have the usual nonlinearity at ~ 17 meV. Both the zero bias anomaly (of varying magnitude and sign) as well as the background are frequently encountered in point contact spectroscopy.[14] The background has been interpreted within the same theoretical framework as the usual peaks,[14] assuming that a nonequilibrium phonon distribution is present near the contact. This implies that it is a bulk effect and therefore should be comprised in the spreading resistance. The physical origin for the zero bias anomaly is not very well established for an arbitrary point contact such as in Fig. 4. Specific studies exist where zero bias anomalies may be explained with scattering processes in the bulk,[23] as well as with interface effects[24] (tunneling junctions). The rectification results for the contacts of Fig. 4 are of interest per se as they support the suggestion that the mechanisms responsible for the zero bias anomaly and the background are of microscopic nature, being inherently fast and not a spurious effect of thermal or other nature.

B. Data as a function of contact resistance

An obviously important experiment to distinguish nonlinearities due to bulk effects (spreading resistance) and tunneling nonlinearities is to investigate contacts of varying resistances. Because the spreading resistance nonlinearity caused by electron-phonon interaction can be unambiguously identified at low temperatures, such data have been taken at liquid helium temperatures. Although the behavior of high-resistance ($\gtrsim 100\ \Omega$) contacts is not very reproducible, a representative set of data is shown in Fig. 5. Only the laser-induced signal curves were recorded and the d^2V/dI^2 was not directly measured. This was found more practical and eliminates the use of the balanced bridge circuit. In the present set up, high-resistance contacts were somewhat difficult to obtain and were very sensitive to ambient mechanical and electrical shocks.

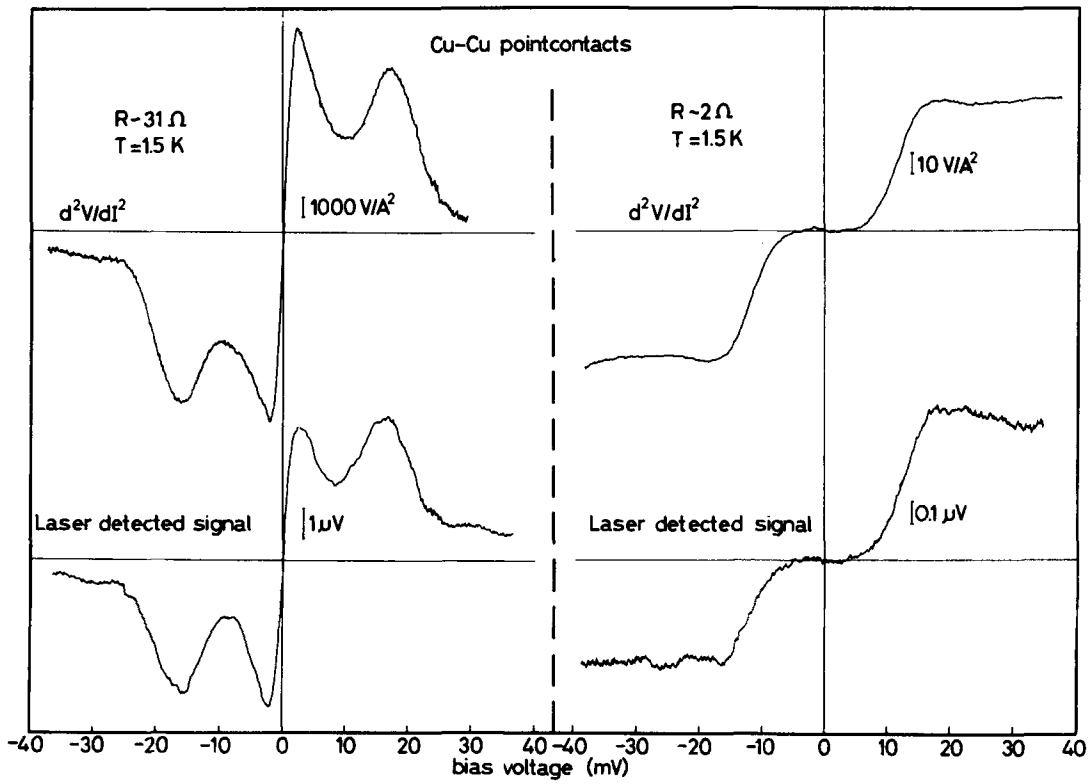

FIG. 4. Second derivative (d^2V/dI^2) and laser-detected signal (V_{det}) curves as a function of bias voltage for a contact with an exceptionally high zero-bias anomaly (left) and a contact with an exceptionally high "background" (right). Laser frequency is 525 GHz in both cases.

The low-resistance contacts ($\lesssim 50\,\Omega$) invariably have the electron phonon interaction peak as the dominant nonlinearity. Higher resistance junctions have a less reproducible behavior, but the phonon scattering induced peaks are still frequently the dominant nonlinearity in contacts of several hundred ohm (see 300 Ω result, Fig. 5). Unfortunately, quantitative measurements of S cannot be made with this detection technique, because the modulation amplitude is unknown. Theoretically, the spreading resistance nonlinearity varies as[14] $S_c \sim R_{FE}^{-\frac{1}{2}}$ for a small constriction and is even smaller for a tunneling junction according to Eq. (3). The laser-induced signal however increases with R_t (for $R_t \lesssim R_a$) according to Eq. (4).

The laser-induced signal for the highest resistance contact in Fig. 5 (lowest trace) has its polarity reversed as compared to the other curves. This is an indication that the nonlinearity is of different origin. Indeed, it is well known that the curvature of an I-V characteristic which is nonlinear due to a tunneling mechanism, is opposite to that caused by the nonlinear spreading resistance as discussed in this work. For nonlinear tunneling mechanisms, the differential resistance decreases with increasing bias voltage. This follows from theory[4,5,8] and is mostly observed experimentally in high-resistance point contacts[4,20] or evaporated tunneling junctions.[25,26] For the presently discussed nonlinearity due to electron phonon interaction, the resistance increases with increasing bias voltage.[14] Some care is required in comparing published high-frequency rectification data (e.g., from Ref. 4), because these are often taken at high power levels (large modulation amplitude). Under that condition, the detected signal is not exclusively determined by the local curvature at the dc-bias point. Calculations of rectification and mixing at

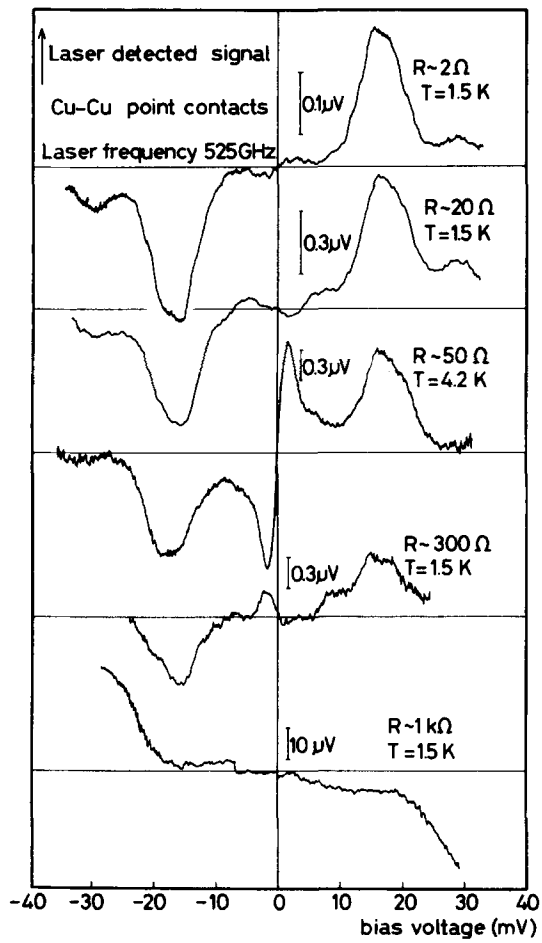

FIG. 5. Laser-detected signal curves as a function of bias voltage for contacts with varying resistances.

large power levels, based on specific parametrizations of the tunneling characteristic[4,5,27–29] have shown that the resulting signals may be of either sign.

From the tunneling models, it is expected that the detected signal for the low power levels and bias voltage regions as in Fig. 5, varies linearly with bias voltage (with negative slope). The lower curve in Fig. 5 is however strongly nonlinear. Comparison with the upper four curves suggests that the observed curve is a superposition of a straight line with negative slope (attributable to the tunneling nonlinearity) and a curve such as the upper one of Fig. 5 (spreading resistance nonlinearity).

The large resistance contacts of Fig. 5 (1 $k\Omega$ and probably also 300 Ω) are almost certainly not of the constriction type, as this would imply unrealistically small constriction diameters (4 Å for 1 $k\Omega$). This fact supports the assignment of some of the observed nonlinearities to tunneling features. Making a plausible estimate for the high-frequency voltage swing in case of the 1 $k\Omega$ contact, together with the observed signal magnitude, leads to an S value smaller (factor 2–5) than would be expected for a (hypothetical) small-constriction 1 $k\Omega$ contact. The difference should then be accounted for by the tunneling probability according to Eq. (3).

The conclusion from Fig. 5 is that the spreading resistance nonlinearity can be dominant even for contacts which presumably are of the tunneling type (300 Ω result). Secondly, spreading resistance nonlinearities and nonlinearities due to tunneling may add independently in the same contact (1 $k\Omega$ result). These observations show that it is useful to distinguish separately nonlinearities due to the barrier resistance and to the spreading resistance.

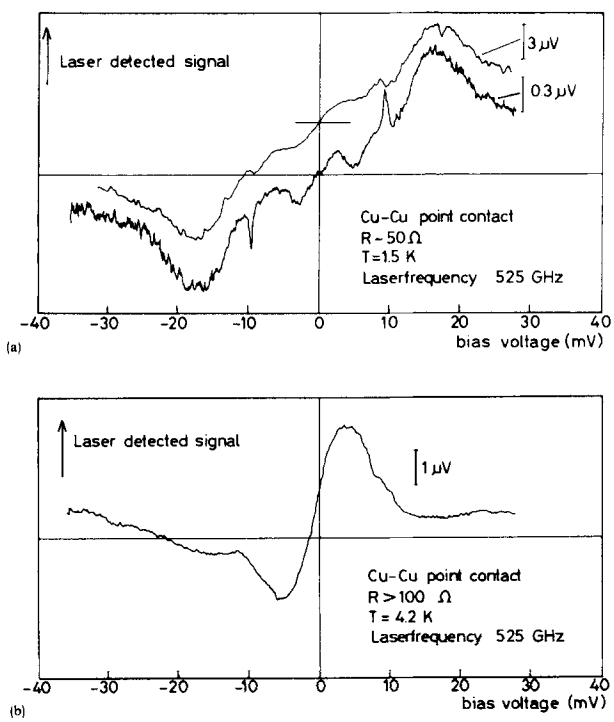

FIG. 6. Laser-detected signal as a function of bias voltage for two different high-resistance contacts showing anomalous behavior. (a) The sharp peaks near 10 mV bias are unexplained; at high power level they are smeared out. (b) Contact with high sensitivity in a low bias voltage region, with finite signal at zero bias.

Figure 6 serves to illustrate the variety of signal shapes, which may accidentally occur in high-resistance contacts. In Fig. 6(a), in addition to the spreading resistance nonlinearity, a narrow peak is superimposed at a bias voltage $\pm$ 10 mV. In the contact of Fig. 6(b), the detected signal is not antisymmetric with respect to zero bias voltage, is relatively large at zero bias, and no effects due to the spreading resistance can be identified. Such anomalous behavior is only observed for high-resistance contacts. This suggests that they should be attributed to an interface effect (oxide-or impurity layer) and therefore to the barrier resitance. Because the nature of the contact is unknown and the behavior can be different from contact to contact, such data are extremely difficult to interpret.

C. Data as a function of temperature

To enable a comparison of the presently described rectification mechanism with room-temperature MIM diodes, measurements have been made at several temperatures (Fig. 7). Both the measured d^2V/dI^2 characteristic and the laser-induced signal plot for the same contact are shown at liquid helium, liquid nitrogen, room temperature, and at $\sim$200 K. For temperatures above 4.2 K, the contact was in ambient gas atmosphere (He) and not in a liquid. The contact had to be readjusted at each temperature. The resistances were chosen in the same order of magnitude and rather low to ensure a small-constriction type contact. The temperature dependence of the I-V characteristics is well known from earlier work[15] and the d^2V/dI^2 curves shown in Fig. 7 are well reprepresentative for it, although taken on different contacts. The distinct structure in d^2V/dI^2 at low temperatures gradually broadens and finally disappears with increasing temperature. The gradual broadening, which tends to a constant level for d^2V/dI^2 at high bias voltage results in a nearly straight line at room temperature over the voltage range displayed. At room temperature, for bias voltages at which the contact remains stable ($\lesssim$ 100 mV), the magnitude of the nonlinearity S is in the same order as that for the "background" at low temperature ($\sim 2\ V^{-1}$). It is to be noted that the sign of d^2V/dI^2 does not change with temperature, i.e., the resistance increases with bias voltage also at room temperature.

As seen from Fig. 7, the laser detected signal curves display precisely the same evolution with temperature as d^2V/dI^2. It can thus be concluded that the effect of the spreading resistance at room temperature is qualitatively similar to that at low temperature. The maximum nonlinearity is however an order of magntiude lower and the characteristic structure is not present.

D. Nonlinearity of W–Ni contact

The combination W–Ni is mostly used for high-frequency MIM diodes. To compare with the previous results for Cu–Cu contacts, the nonlinearity (d^2V/dI^2) for a typical low resistance W–Ni contact was measured at liquid helium and at room temperature (see Fig. 8). A standard W whisker,

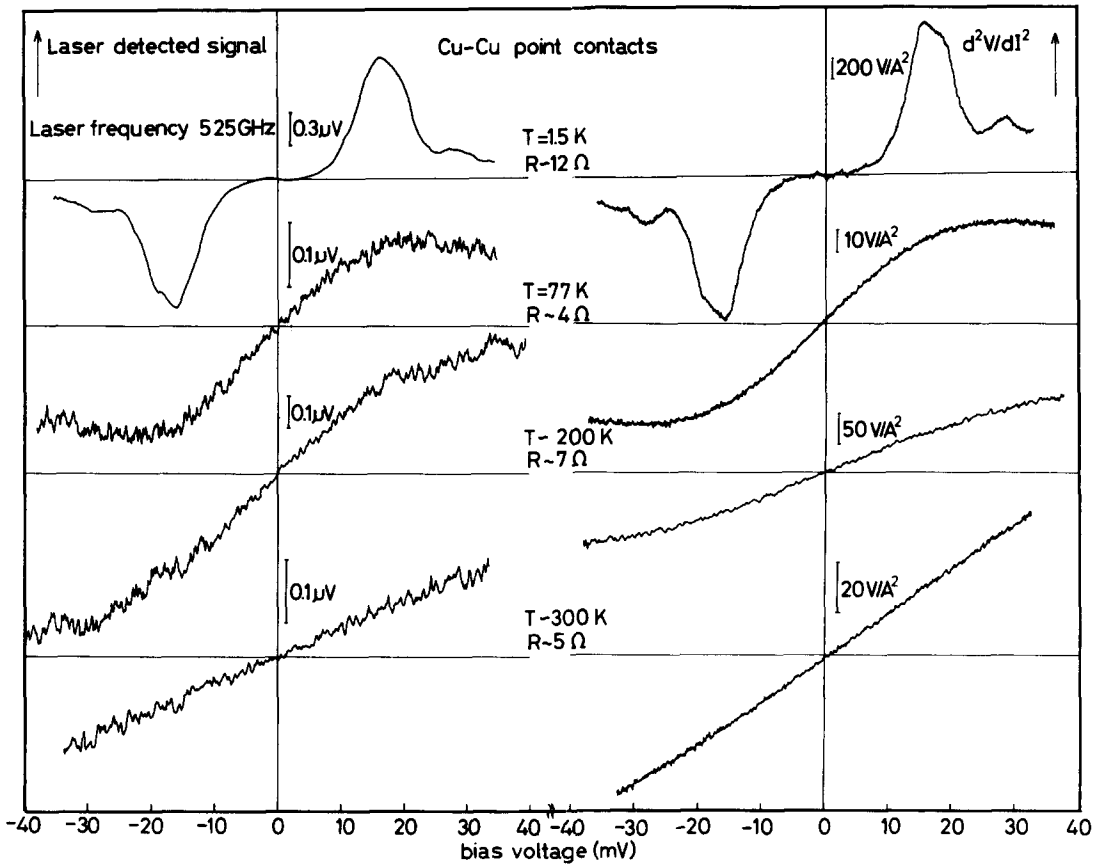

FIG. 7. Laser-detected signal curves (left) and second derivative (d^2V/dI^2) curves (right) as a function of bias voltage at different temperatures. For each temperature, the contact was newly adjusted.

as used in our laboratory in a microwave harmonic generator,[30] was used as the point electrode. The Ni post was from reasonable purity, but further arbitrary material. The low temperature result [Fig. 8(a)] indeed shows the electron phonon scattering induced nonlinearities, with the known spectra of W[31] and Ni[32] presumably superimposed.

A peculiarity of contacts with Ni as one of the electrodes is however that often also a strong and sharp nonlinearity occurs at high bias voltages ($\sim$200 mV). Such a nonlinearity was earlier observed at liquid helium temperatures,[32] but appears to be present also at room temperature [see Fig. 8(b)]. Its origin was attributed to heating near the ferromagnetic transition temperature of Ni.[32] This nonlinearity has not been investigated further, but would certainly provide an extra complication in an analysis of low-resistance W–Ni contacts. As its presence has been attributed to heating, the high-frequency behavior might be different from low-frequency behavior.

E. Expected high-frequency cutoff

An evaluation of the relative importance of the spreading resistance nonlinearity is incomplete, until its effective frequency range is known. Fundamental cutoffs, as a result of the intrinsic speed of the physical mechanism behind the nonlinearity, must be distinguished from cutoffs due to circuit effects. Circuit effects lead in general to a power law rolloff, so that a diode may be operated above cutoff (with consequent reduction in response). From the simple circuit of Fig. 2, with R_s the nonlinear resistance, the response would be expected to be frequency independent when R_b is shorted by C. As remarked already however, the operation principle for the nonlinear R_s will be affected when R_b is shorted. Therefore, the frequency rolloff at frequencies $\omega > 1/R_bC$ cannot be deduced from the circuit of Fig. 2. Operation above this cutoff frequency is uncertain.

The fundamental frequency cutoff for the presently discussed mechanism is determined by the average electron phonon relaxation time constant τ, determined by the phonons of maximum energy. Its value is in the order 10^{-13}–10^{-14} sec typically. A prerequisite is that the phase of the high-frequency field does not change sign during passage of an electron through the field region. For a small constriction, it is in the order $a/v_F \lesssim 10^{-14}$ sec, for a tunneling junction in the order of 10^{-15} sec.[4]

A reasonable estimate for C from estimates of contact area ($\sim 10^{-2}\,\mu m^2$) and dielectric layer thickness ($\sim$1 nm)[21] yields $C \sim 10^{-15}$ F. For the typical contact resistances (10–100 Ω) the circuit cutoff occurs in about the same frequency range as the fundamental cutoff. The maximum frequency for which the mechanism is operational therefore is between 10^{13} and 10^{14} Hz.[33]

V. DISCUSSION

In this section, a quantitative comparison will be made of the metal-metal contact whose nonlinearity is dominated by the spreading resistance with literature data on MIM contacts. Although practical interest in high-frequency point contact devices is in harmonic generation and mixing, these

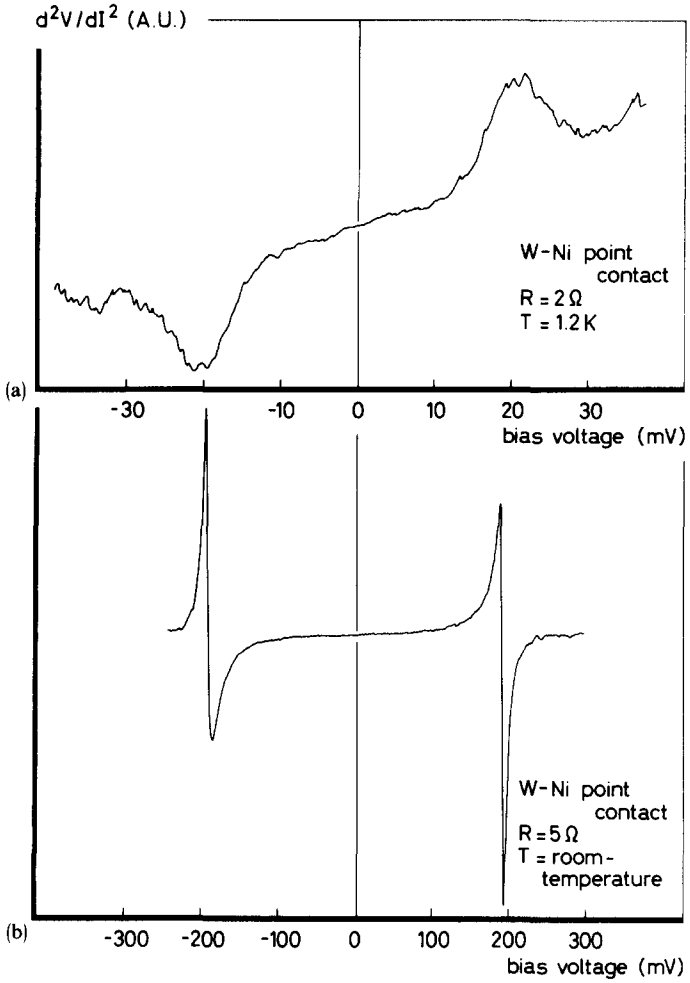

FIG. 8. Second derivative (d^2V/dI^2) curves of two W–Ni point contacts. The upper curve is taken at ~1.2 K and displays the usual structure of a constriction-type point contact. The lower curve is taken at room temperature and exhibits very strong nonlinearities near 200 mV bias voltage.

properties are hard to evaluate and difficult to compare. Therefore only video detection properties will be compared, assuming that this is a reasonable relative measure for all high-frequency properties. Operation below cutoff will be assumed.

To select a typical contact, a small-constriction type is chosen, since for this one the spreading resistance nonlinearities are maximal [from Eq. (3)]. From Eq. (4), it follows that the sensitivity increases with $R_t^{3/2}$. As shown, for too high resistances, other types of nonlinearities occur. Therefore we choose as a reasonable value $R_t = 20\ \Omega$.

Using the typical values $R_t = 20\ \Omega$, $R_a = 150\ \Omega$, $S = 10\ \mathrm{V}^{-1}$ (at liquid helium temperature), a sensitivity of 40 V/W follows from Eq. (4). A more useful measure for the sensitivity of a video detector is the noise equivalent power (NEP) in $\mathrm{W}/\sqrt{\mathrm{Hz}}$. Assuming shot noise to be dominant at finite bias voltage, the NEP can be expressed as $\mathrm{NEP} = \sqrt{2eI}/\frac{1}{2}SF$ with F the impedance mismatch factor. Using the same parameters and $I = 17\ \mathrm{mV}/20\ \Omega$, one obtains $\mathrm{NEP} \sim 10^{-11}\ \mathrm{W}/\sqrt{\mathrm{Hz}}$. This value does not include the coupling efficiency of radiation at the antenna, which was poor in the present setup. At room temperature the NEP will be an order of magnitude higher.

Some care is required in comparing the quoted NEP value with similar estimates for conventional room temperature MIM diodes. In practical cases, they are usually operated without external bias. Literature values for S at zero bias scatter by several orders of magnitude. From systematic investigations of the I-V characteristic, $S(V = 0)$ appears to be generally a negligible fraction of the value at some optimum finite bias.[4,20] A comparison of estimated sensitivities of typical diodes, as may be inferred from literature data, is given in Table I. In Ref. 21, an NEP value was given for the usual room temperature operating condition. Because Johnson noise was assumed to limit the NEP, the value would be lower if the diode were operated at 4.2 K, assuming that the diode parameters remain unchanged. Using parameters for the diode described in Ref. 20 and assuming shot noise, an NEP value is obtained for a biased, room temperature MIM-diode. From Table I, it appears that the sensitivity of the low temperature constriction point contact is certainly comparable or perhaps superior to the best values which may be obtained for MIM diodes, even if they were operated at low temperature, with or without bias. It should be added that the estimated performance for the constriction contact is obtained for a low resistance contact ($\sim 20\ \Omega$), whereas for the typical tunneling contacts the resistance is high ($\sim 1\ k\Omega$). A low-resistance contact is generally more stable than a high-resistance contact.

The primarily relevant frequency range for MIM di-

TABLE I. Comparison of different diode types.

Diode type	Operating temperature	Bias voltage	NEP ($\mathrm{W}/\sqrt{\mathrm{Hz}}$)	Remarks
Present	4.2 K	yes	10^{-11}	shot noise
	room temp.	yes	10^{-10}	assumed
MIM, Ref. 21	room temp.	no	10^{-10}	Johnson noise
	4.2 K	no	$\lesssim 10^{-11}$	assumed
MIM, Ref. 20	room temp.	yes	$\lesssim 10^{-11}$	shot noise assumed
Schottky diode Ref. 34	room temp.	yes	10^{-8}	measured value (Ref. 34), not corrected for coupling losses

odes is at near infrared or higher. The nonlinearity of the constriction type contact seems not of much use in this frequency range which is above the expected high-frequency cutoff. At lower frequencies, the Schottky diode (operating at room temperature) has been used successfully over the entire far-infrared range[34] and will perhaps operate at frequencies as high as 30 THz.[35] For a Schottky diode, a typical measured NEP value is 10^{-8} W/$\sqrt{\text{Hz}}$[34] at FIR frequencies. Even after correction for antenna coupling losses, this value seems not to be superior to the theoretically estimated values for the low-temperature constriction contact. At low temperatures and in the far-infrared region, the sensitive superconducting devices (Josephson junctions[36]) should be considered at first for heterodyne experiments or harmonic mixing.

VI. CONCLUSION

High-frequency rectification by metal-metal point contacts has been investigated at far-infrared frequencies. The results have been interpreted using the conventional model of the point contact resistance, separating it in a spreading resistance and a barrier resistance. In particular, the relative importance of the spreading resistance nonlinearity was investigated. This nonlinearity is due to electron phonon interaction processes in the bulk material and can be well identified at low temperatures.

In low-resistance contacts ($\lesssim 50\,\Omega$) the spreading resistance nonlinearity is dominant at all temperatures. In higher resistance contacts, another type of nonlinearity also may determine the response. The mechanism responsible for this nonlinearity is presumably associated with electron tunneling, as usually assumed in the analysis of MIM junctions. In the high-resistance contacts ($50\,\Omega < R < 1\,k\Omega$) both types of nonlinearities can coexist independently, while either one may be dominant.

The high-frequency cutoff, associated with the spreading resistance nonlinearity is expected to be lower than the potentially interesting frequency range for applications. At lower frequencies however, using this nonlinearity, sensitivities may be obtained comparable with or better than with existing devices (MIM-diodes, Schottky diodes).

ACKNOWLEDGMENTS

We are most grateful to Dr. A. G. M. Jansen for helpful discussions. The tunable CO_2 laser used to pump the far-infrared laser was developed in our laboratory and is one of a series which was built for commercial purposes by the workshop of the Faculty of Science of the University of Nijmegen. This work is part of the research program of the Stichting voor Fundamenteel Onderzoek der Materie (Foundation for Fundamental Research on Matter) and was made possible by financial support from the Nederlandse Organisatie voor Zuiver-Wetenschappelijk Onderzoek (Netherlands Organization for the Advancement of Pure Research).

[1]For recent reviews see K. M. Evenson and F. R. Petersen, in *Laser Spectroscopy of Atoms and Molecules*, edited by H. Walther (Springer, Berlin, 1976); J. J. Jimenez and F. R. Petersen, Infrared Phys. **17**, 541 (1977).

[2]L. M. Matarrese and K. M. Evenson, Appl. Phys. Lett. **17**, 8 (1970); B. L. Twu and S. E. Schwarz, Appl. Phys. Lett. **26**, 672 (1975).

[3]For a comparative review see D. J. E. Knight and P. T. Woods, J. Phys. E **9**, 898 (1976).

[4]S. M. Faris, T. K. Gustafson, and J. C. Wiesner, IEEE J. Quantum Electron **QB-9**, 737 (1973).

[5]J. G. Simmons, J. Appl. Phys. **34**, 2581 (1963); S. P. Kwok, G. I. Haddad, and G. Lobov, J. Appl. Phys. **42**, 554 (1971); S. M. Faris and T. K. Gustafson, Appl. Phys. Lett. **25**, 544 (1974).

[6]N. M. Miskovsky, P. H. Cutler, T. E. Feuchtwang, and A. A. Lucas, Int. J. Infrared Millimeter Waves **2**, 739 (1981) and references therein.

[7]H.-U. Daniel, M. Steiner, and H. Walther, Appl. Phys. **25**, 7 (1981).

[8]N. M. Miskovsky, P. H. Cutler, T. E. Feuchtwang, and A. A. Lucas, Appl. Phys. A **27**, 139 (1982).

[9]G. M. Elchinger, A. Sanchez, C. F. Davies, Jr., and A. Javan, J. Appl. Phys. **47**, 591 (1976).

[10]H. D. Riccius, Infrared Phys. **17**, 245 (1977); H. D. Riccius, Appl. Phys. **24**, 215 (1981).

[11]D. P. Siu and T. K. Gustafson, Appl. Phys. Lett. **31**, 71 (1977); D. P. Siu, R. K. Jain, and T. K. Gustafson, Appl. Phys. Lett. **28**, 407 (1976).

[12]R. W. Van der Heijden, A. G. M. Jansen, J. H. M. Stoelinga, H. M. Swartjes, and P. Wyder, Appl. Phys. Lett. **37**, 245 (1980).

[13]I. K. Yanson, Zh. Eksp. Teor. Fiz. **66**, 1035 (1974) [Sov. Phys. JETP **39**, 506 (1974)]; A. G. M. Jansen, F. M. Mueller, and P. Wyder, Phys. Rev. B **16**, 1325 (1977).

[14]For a review see A. G. M. Jansen, A. P. van Gelder, and P. Wyder, J. Phys. C **13**, 6073 (1980); A. G. M. Jansen, thesis, University of Nijmegen, 1980.

[15]A. P van Gelder, A. G. M. Jansen, and P. Wyder, Phys. Rev. B **22**, 1515 (1980).

[16]R. Holm, *Electric Contacts* (Springer, Berlin, 1967).

[17]Yu. V. Sharvin, Zh. Eksp. Teor. Fiz. **48**, 984 (1965) [Sov. Phys. JETP **21**, 655 (1965)].

[18]I. O. Kulik, A. N. Omel'yanchuk, and R. I. Shekhter, Fiz. Nizk. Temp. **3**, 1543 (1977) [Sov. J. Low Temp. Phys. **3**, 740 (1977)]; A. P. van Gelder, Solid State Commun. **25**, 1097 (1978).

[19]C. C. Bradley and G. J. Edwards, IEEE J. Quantum Electron. **QE-9**, 548 (1973).

[20]B. L. Twu and S. E. Schwarz, Appl. Phys. Lett. **25**, 595 (1974).

[21]A. Sanchez, C. F. Davis, Jr., K. C. Liu, and A. Javan, J. Appl. Phys. **49**, 5270 (1978).

[22]Y. Yasuoka, T. Sakurada, D. P. Siu, and T. K. Gustafson, J. Appl. Phys. **50**, 5860 (1979).

[23]A. G. M. Jansen, A. P. van Gelder, P. Wyder, and S. Strässler, J. Phys. F **11**, L15 (1981).

[24]E. L. Wolf, in *Inelastic Electron Tunneling Spectroscopy*, edited by T. Wolfram (Springer, Berlin, 1978).

[25]T. K. Gustafson, R. V. Schmidt, and J. R. Perucca, Appl. Phys. Lett. **24**, 620 (1974).

[26]M. Heiblum, S. Wang, J. R. Whinnery, and T. K. Gustafson, IEEE J. Quantum Electron. **QE-9**, 548 (1973).

[27]S. M. Faris, B. Fan, and T. K. Gustafson, Appl. Phys. Lett. **27**, 629 (1975).

[28]B. Fan, S. M. Faris, T. K. Gustafson, and T. J. Bridges, Appl. Phys. Lett. **30**, 177 (1977).

[29]S. I. Green, P. D. Coleman, and J. R. Baird, presented at the Symposium on Submillimeter Waves, Polytechnic Institute of New York, Brooklyn, 1970, pp. 369–389.

[30]M. J. Huyben, C. G. C. M. de Kort, J. H. M. Stoelinga, and P. Wyder, Infrared Phys. **19**, 257 (1979).

[31]A. G. M. Jansen, doctoral thesis, University of Nijmegen, 1976; J. Caro, R. Coehoorn, and D. G. de Groot, Solid State Commun. **39**, 267 (1981).

[32]B. I. Verkin, I. K. Yanson, I. O. Kulik, and O. I. Shklyarevski, Solid State Commun. **30**, 215 (1978).

[33]At these high frequencies, in fact a quantum treatment of rectification should be employed: J. R. Tucker and M. F. Millea, Appl. Phys. Lett. **33**, 611 (1978). Quantum effects already start to play a role at frequencies of a few THz.

[34]H. R. Fetterman, B. J. Clifton, P. E. Tannenwald, and C. D. Parker, Appl. Phys. Lett. **24**, 70 (1974); D. T. Hodges and M. McColl, Appl. Phys. Lett. **30**, 5 (1977); B. F. J. Zuidberg and A. Dymanus, Appl. Phys. Lett. **29**, 643 (1976); D. D. Bicanic, B. F. J. Zuidberg, and A. Dymanus, Appl. Phys. Lett. **32**, 367 (1978).

[35]D. Tsang and S. E. Schwarz, Appl. Phys. Lett. **30**, 263 (1977).

[36]P. L. Richards, in *Semiconductors and Semimetals*, Vol. 12, edited by R. K. Willardson and A. C. Beer (Academic, New York, 1977) pp. 395–439.